Natural convection in horizontal annulus filled with an anisotropic porous medium

K. Aboubi, L. Robillard and P. Vasseur

Department of Mechanical Engineering, Ecole Polytechnique, University of Montreal, Montreal, Quebec, Canada

Received September 1995
Revised June 1996 and April 1997
Accepted March 1998

Nomenclature

A = added resistivity tensor due to anisotropy
$\vec{g}$ = terrestrial gravity
$\hat{g}$ = unit vector in the downward direction
I = identity matrix
k = thermal conductivity of the satured porous medium, $[Wm^{-1}\,K^{-1}]$
K = permeability tensor of the anisotropic porous medium, $[m^2]$
K_1, K_2 = extreme values of permeability defining the principal axes, $[m^2]$
K^* = permeability ratio, K_1/K_2
Nu = overall Nusselt number defined by equation (13)
P = overall hydraulic resistivity tensor
p = dimensionless pressure
R = radius ratio, r_2'/r_1'
Ra = Rayleigh number, $K_1\, g\eta\Delta\, T' r_1'/\nu\alpha$
Ra^* = modified Rayleigh number, $Ra/\sqrt{K^*}$
r = dimensionless radial coordinate
t = dimensionless time
T = dimensionless temperature
$\Delta T'$ = characteristic temperature difference
u, v = dimensionless velocity components in r and φ directions
$\vec{V}$ = dimensionless velocity vector

Greek symbols

α = thermal diffusivity, $(k/(\rho c)_f)$ $[m^2\,s^{-1}]$
γ = angular coordinate of the principal axis corresponding to K_1
η = thermal expansion coefficient $[K^{-1}]$
μ = dynamic viscosity of the fluid $[kg\,m^{-1}\,s^{-1}]$
ν = kinematic viscosity of the fluid $[m^2\,s^{-1}]$
ρ = density of the fluid $[kg\,m^{-3}]$
$(\rho c)_f$ = heat capacity of the fluid $[J\,m^{-3}K^{-1}]$
$(\rho c)_p$ = heat capacity of the saturated porous medium $[J, m^{-3}\,K^{-1}]$
σ = heat capacity ratio $(\rho c)_p/(\rho c)_f$
φ = angular coordinate
ψ = dimensionless stream function

Superscripts

$'$ = dimensional variable

Subscripts

1 = value on inner cylinder
2 = value on outer cylinder

Other symbols

∇^2 = Laplacian operator $(\nabla^2 = \frac{1}{r}\frac{\partial}{\partial r}(r\frac{\partial}{\partial r}) + (\frac{1}{r^2}\frac{\partial^2}{\partial \varphi^2})$

Introduction

Natural convection in a horizontal annular space filled with a porous material has received considerable attention in the past. The interest in this basic configuration has been stimulated, to a large extent, by the fact that this geometry is of importance in the field of thermal insulating engineering. Much of the activity on this topic, both numerical and experimental, has been summarized in a recent book by Nield and Bejan (1992) . From this review of the literature it is clear that so far, investigations have been concerned solely with isotropic porous media. The case of an anisotropic porous horizontal annulus, which is encountered in engineering practices, has not been studied. Earlier

Financial support by Natural Sciences and Engineering Research Council of Canada and FCAR of Province of Quebec are acknowledged.

International Journal of Numerical Methods for Heat & Fluid Flow
Vol. 8 No. 6, 1998, pp. 689–702.

studies on natural convection in a saturated anisotropic porous medium are concerned mostly with the case of horizontal layer heated from below (see for instance Ephere(1977) and Kvernvold and Tyvand (1979)). Castinel and Combarnous (1977) have analyzed the case of inclined layers while Burns *et al.* (1977) have examined natural convection in a vertical slot filled with an anisotropic porous medium. In those two studies, the porous medium was taken to be thermally isotropic. The anisotropy of both permeability and thermal conductivity was considered by Ni and Beckermann (1991), Degan and Vasseur (1996; 1997) Degan *et al.* (1995) for the case of a rectangular cavity and by Chang and Hsiao (1993) for the case of a vertical cylinder.

The present investigation deals with the two-dimensional natural convection in a horizontal annulus filled with an anosotropic porous medium. In a way similar to Patil *et al.* (1989), anisotropy in permeability is considered with principal axes oriented at a constant but arbitrary angle with respect to the vertical direction. The inner and outer boundaries of the flow domain are isothermal with the outer one being warmer. The problem is formulated in terms of Darcy-Boussinesq approximation and solved numerically, using a time-marching finite-difference method, until a steady state is reached. Effects of various parameters, such as the Rayleigh number Ra^*, the permeability ratio K^* and the angular position γ of the principal axes are analyzed. By contrast with previous works on the same geometry, dealing with isotropic porous media, such as the one by Caltagirone (1976) or Kaviany (1986), the arbitrary inclination of the principal axes in the present investigation does not allow the use of a symmetry hypothesis with respect to the vertical diameter and consequently the whole annulus must be taken as flow domain (doubly-connected domain) with the possibility of a net flow circulating between the two boundaries.

Statement of the problem

Governing equations are expressed in the polar coordinate system, shown in Figure 1. The flow domain is limited by two concentric horizontal cylinders of radius r'_1 and r'_2, and consists of a fluid saturated anisotropic porous medium with principal axes defined by the extreme permeabilities K_1 and K_2.The principal axes are in the same direction for all the points of the flow domain, i.e. the angle γ with the origin keeps the same value at any position (r, φ). The inner and outer boundaries are at isothermal temperatures T'_1 and T'_2, respectively, with $T'_2 > T'_1$.

With the use of the Boussinesq approximation, the generalized momentum equation for anisotropic porous media (Bear, 1972) becomes in dimensionless form:

$$\mathbf{P}\,\vec{V} = -\nabla p - RaT\hat{g} \tag{1}$$

in which $Ra = K_1\,\hat{g}\,\eta\Delta T' r'_1/\nu\alpha$, is the porous medium Rayleigh number, $\mathbf{P} = \mathbf{K}^{-1}$, a second order resistivity tensor and $\hat{g}$, a unit vector in the downward (gravity) direction. Variables, $\vec{V}$, p and T are the velocity vector, dynamic pressure and

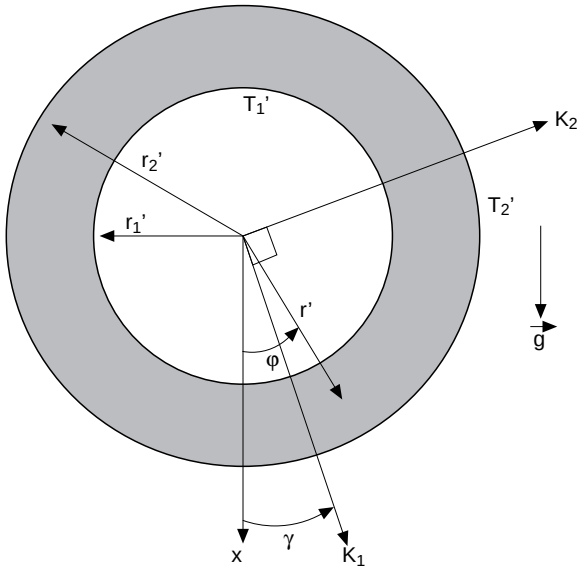

Figure 1.
Geometry of the problem

temperature respectively. Those have been made dimensionless by using the scales r_1', $\alpha r_1'$, $\alpha\mu/K_1$ and $\Delta T' = T_2' - T_1'$ for length, velocity, pressure and temperature respectively. All other symbols are defined in nomenclature.

For two-dimensional motion, **P** takes the form:

$$\mathbf{P} = \begin{Bmatrix} \cos^2\beta + K^* \sin^2\beta & (K^*-1)\dfrac{\sin 2\beta}{2} \\ (K^*-1)\dfrac{\sin 2\beta}{2} & \sin^2\beta + K^*\cos^2\beta \end{Bmatrix} \tag{2}$$

in which $\beta = \varphi - \gamma$ and $K^* = K_1/K_2$. The resistivity tensor in equation (2) is already dimensionless. It may be split in the sum of two terms:

$$\mathbf{P} = \mathbf{I} + (K^*-1)\,\mathbf{A} = \begin{bmatrix} 1 & 0 \\ 0 & 1 \end{bmatrix} + (K^*-1) \begin{bmatrix} \sin^2\beta & \dfrac{\sin 2\beta}{2} \\ \dfrac{\sin 2\beta}{2} & \cos^2\beta \end{bmatrix} \tag{3a}$$

For $K^* > 1$, the first term **I** (identity matrix) represents the isotropic resistivity based on the maximum permeability K_1, (i.e. minimum resistivity) and the second term A is the added resistivity due to anisotropy. If $K^* < 1$, one can renormalize equation (3a), by dividing it by K^*. The permeability K_2, which now corresponds to the maximum permeability, replaces K_1 in the Rayleigh number and pressure scale while a new resistivity tensor of the form:

$$\frac{\mathbf{P}}{K^*} = \begin{bmatrix} 1 & 0 \\ 0 & 1 \end{bmatrix} + \left(\frac{1}{K^*} - 1\right) \begin{bmatrix} \cos^2\beta & -\frac{\sin 2\beta}{2} \\ -\frac{\sin 2\beta}{2} & \sin^2\beta \end{bmatrix} \tag{3b}$$

replaces **P** on the left hand side. The differences found in the second term of (3b) are due to the shift by 90° of the minimum resistivity (or maximum permeability).

It is worth noticing that the second term in equation (3a) or in equation (3b) is equivalent, under some restrictions, to the added resistivity of a magnetic field $\vec{B}$ acting on a porous medium saturated with a conducting fluid (see Appendix).

Other dimensionless governing equations are the continuity and energy equations:

$$\nabla \cdot \vec{V} = 0 \tag{4}$$

$$\frac{\partial T}{\partial t} + u\frac{\partial T}{\partial r} + \frac{v}{r}\frac{\partial T}{\partial \varphi} = \frac{1}{r}\frac{\partial}{\partial r}\left(r\frac{\partial T}{\partial r}\right) + \frac{1}{r^2}\frac{\partial^2 T}{\partial \varphi^2} \tag{5}$$

with boundary conditions:

$$\begin{aligned} r = 1: &\qquad u = 0, \qquad T = 0 \\ r = R: &\qquad u = 0, \qquad T = 1 \end{aligned} \tag{6}$$

The pressure gradient is eliminated by taking the curl of equation (1). We obtain:

$$\begin{aligned} \nabla^2\psi + (1 - K^*)\Bigg[&\cos^2\beta \frac{1}{r}\frac{\partial}{\partial r}\left(r\frac{\partial \psi}{\partial r}\right) + \sin^2\beta \frac{1}{r^2}\frac{\partial^2 \psi}{\partial \varphi^2} \\ &- \sin 2\beta \frac{1}{r}\frac{\partial^2 \psi}{\partial r \partial \varphi} - \cos 2\beta \frac{1}{r}\frac{\partial \psi}{\partial r} + \sin 2\beta \frac{1}{r^2}\frac{\partial \psi}{\partial \varphi}\Bigg] \\ &= -Ra\left(\frac{\partial T}{\partial r}\sin\varphi + \frac{1}{r}\frac{\partial T}{\partial \varphi}\cos\varphi\right) \end{aligned} \tag{7}$$

where ψ is the stream function related to the velocity components by:

$$u = \frac{1}{r}\frac{\partial \psi}{\partial \varphi} \qquad v = -\frac{\partial \psi}{\partial r} \tag{8}$$

Here also, the left-hand side part of equation (7) is split into isotropic and anisotropic terms.

The two circular boundaries define a doubly-connected region. As mentioned earlier, one must allow for the possibility of a net circulating flow between the two boundaries. Appropriate boundary conditions for ψ and T are:

$$\begin{array}{lll} r=1 & \psi=\psi_1 & T=0 \\ r=R & \psi=0 & T=1 \end{array} \tag{9}$$

with ψ_1 corresponding to an unknown net circulating flow around the annulus. An additional condition is required to find ψ_1. This condition is found by integrating the φ component of equation (1) over $0 \le \varphi \le 2\pi$ and $0 \le r \le R$, and by using the following periodicity condition:

$$f(r,\varphi) = f(r,\varphi + 2\pi) \tag{10}$$

where f stands for any physical variable, to eliminate some terms. We obtain:

$$\psi_1 = \frac{1}{\pi(K^*+1)} \int_0^{2\pi} \int_1^R [\, RaT \sin\varphi - \frac{(K^*-1)}{2} u \sin 2\beta \,]\, dr d\varphi \tag{11}$$

Equations (5), (7) and (8), together with boundary conditions (9) and (11) are to be solved numerically. The governing parameters are Ra, R, γ and K^*.

If $\psi(r, \varphi)$ and $T(r, \varphi)$ are solutions at (Ra, R, γ, K^*), they are also solutions at (Ra, R, $\gamma + \pi$, K^*) and $-\psi(r, \varphi)$ and $T(r, -\varphi)$ are solutions at (Ra, R, $-\gamma$, K^*). Consequently the investigation may be limited to the range $0 \le \gamma \le \pi/2$.

A modified Rayleigh number of the form:

$$Ra^* = \frac{g\eta \Delta T' r_1' \sqrt{K_1/K_2}}{\nu\alpha} = Ra/\sqrt{K^*} \tag{12}$$

is more appropriate to describe the results. The two extreme permeabilities K_1 and K_2 have the same weight in the definition (12) and it is consequently possible to isolate in a better way the effects of the permeability ratio from other effects normally attributed to a change in Rayleigh number. Moreover, with the definition (12), it can be deduced that if $\psi(r, \varphi)$ and $T(r, \varphi)$ are solutions at (Ra^*, R, γ, K^*), so they are at (Ra^*, R, $\gamma + \pi/2$, $1/K^*$).

An overall Nusselt number defined as:

$$Nu = \frac{\ln R}{2\pi} \int_0^{2\pi} \left.\frac{\partial T}{\partial r}\right|_{r=1} d\varphi = \frac{\ln R}{2\pi} \int_0^{2\pi} \left.\frac{\partial T}{\partial r}\right|_{r=R} R d\varphi \tag{13}$$

is used to describe the heat transfer from one boundary to the other. The value $2\pi/\ln R$ corresponds to the pure conduction heat transfer.

Numerical study

Numerical solutions of the governing equations are obtained by a finite-difference method. A successive overrelaxation method is used to solve equation (7). The energy equation, in its time dependent form (5) is solved by an alternating direction implicit method (ADI). The ADI approach in the φ direction is based on the fact that any physical variable f should satisfy periodic condition (10). All derivatives are discretized according to the Taylor-based second order central difference scheme for a regular mesh size. The value of the

stream function on the inner boundary is found by numerically evaluating the integral (11) with a trapezoidal rule computation.

Some results for the isotropic case were obtained from the present numerical approach and a comparison with those reported by Caltagirone (1976) is shown in Table I.

Grid tests were done at $R = 2$, covering the range $0 < Ra^* < 300$. Since comparisons between (18×36) and (36×72) mesh sizes gave results that were practically identical for the range of Ra^* considered in this study, the (18×36) mesh size was adopted for all results. The governing coupled equations (7) and (5) are solved iteratively with a time step of $\Delta t = 510^{-4}$ until the steady state is reached.

Results and discussion

It is first instructive to examine the ranges of the governing dimensionless parameters Ra^*, K^*, γ and R considered in the present study. Results are presented for Rayleigh numbers $Ra^* = 100$, 150 and 200, a permeability ratio K^* ranging from 0.1 to 10, and the angular position of the principal axes γ ranging from 0 to $\pi/2$. The radius ratio is held fixed at R = 2.

The behavior of flow and temperature fields and the heat transfer rate may be better understood by observing the evolution of the flow patterns obtained when a single parameter is changed at a time. For instance, the set of Figures 2(a-c) shows flow (at left) and temperature fields (at right) by streamlines and isotherms respectively, for different values of the permeability ratio K^*, while γ and Ra^* are maintained at 0 and 200, respectively. In those figures, the direction and relative importance of the maximum and minimum permeabilities are illustrated by the angular position and relative lengths of the perpendicular lines shown at the center of the annulus. The sequence of figures evolves from top to bottom with the first figure having the maximum permeability in the vertical direction and the last one having the maximum permeability in the horizontal direction. Figure 2(b) shows flow and temperature fields for $K^* = 1$ (isotropic porous medium). Those fields, which are practically identical to those shown in the article by Caltagirone, are given for comparison purpose. Following the definition (12), the solution shown in Figure 2(a) is equivalent to the one obtained for $Ra^* = 200$, $\gamma = 90°$ and $K^* = 0.125$. All flow and temperature fields shown in Figure 2 are symmetrical with respect to the vertical diameter and no net circulating flow exists around the annulus ($\psi_1 = 0$). The flow pattern shown in Figure 2(a) has a particular feature. The

Table I.
Results of the isotropic case compared with those of Caltagirone (1976)

	Caltagirone (1976)		Present approach	
Ra	Nu	ψ_{max}	Nu	ψ_{max}
25	1.099	2.892	1.099	2.904
50	1.328	5.493	1.332	5.560
100	1.828	9.748	1.847	9.963
200	2.625	15.859	2.661	16.35

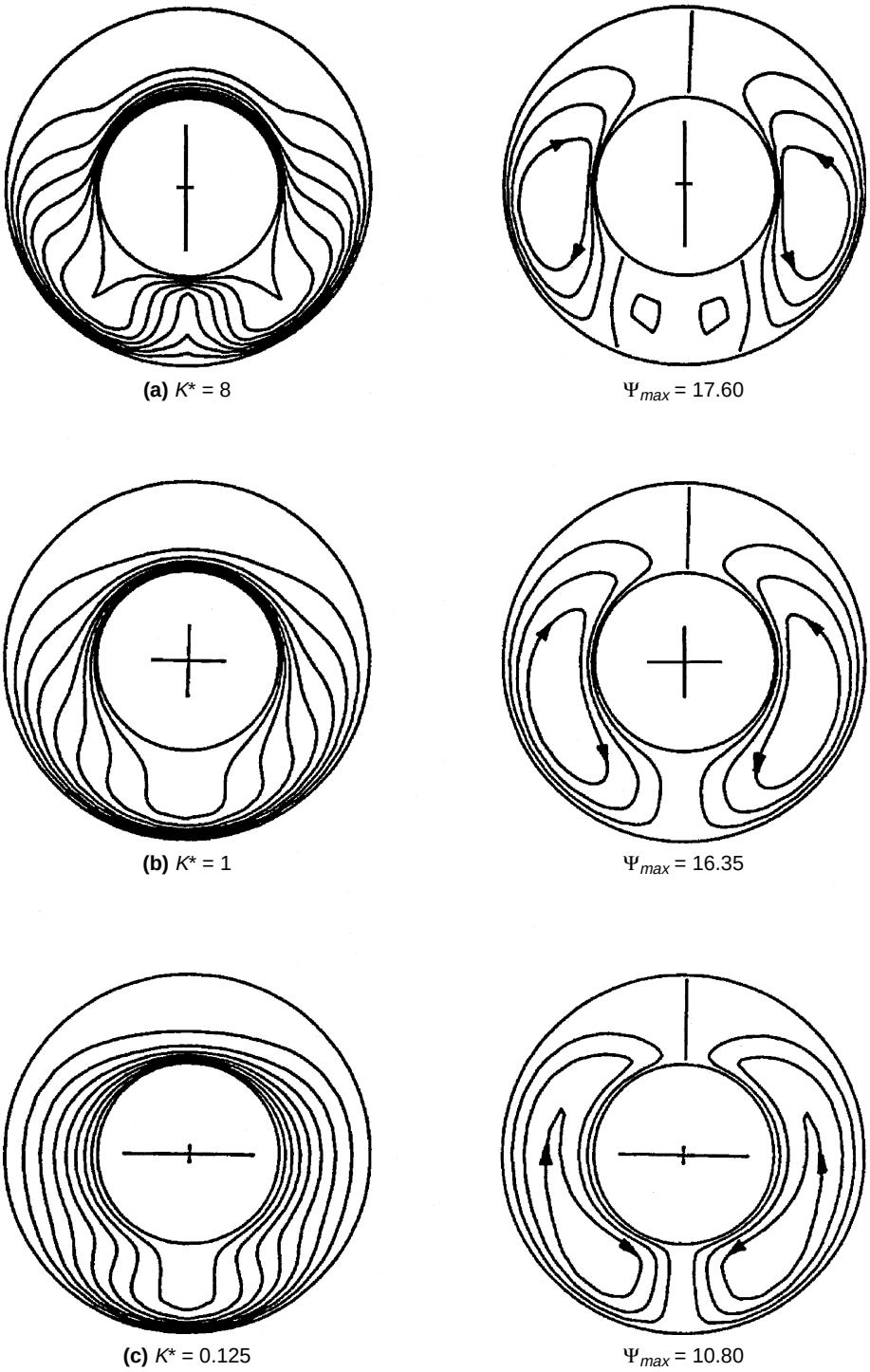

Figure 2.
Effect of permeability ration K^* on the flow and temperature fields for $Ra^* = 200$ and $\gamma = 0°$

permeability being small in the horizontal direction, a greater resistance is offered to the fluid in that direction by the solid matrix and, as a consequence, the unstable layer at the lower part of the annulus generates two additional (secondary) convection cells. Those secondary cells would also occur for an isotropic medium for $R \rightarrow 1$.

Figure 3 shows the temperature and flow fields obtained by increasing the value of the Rayleigh number Ra^* while maintaining constant γ and K^*. The left column displays isotherms and the right one displays streamlines for $\gamma = 0°$ and $K^* = 0.25$. For small Rayleigh numbers such as the one of Figure 2(a), the isotherms are weakly disturbed from the concentric (pseudo-conduction) pattern. As Ra^* increases, the convective motion becomes more important and the isotherms produce steep gradients near the wall in the bottom region ($\varphi = 0°$) and in the upper region ($\varphi = 90°$) for the outer and inner boundaries respectively.

Figure 4 shows the overall Nusselt number Nu, defined in equation (13), as a function of the permeability ratio K^* for $Ra^* = 100$, 150 and 200 and $\gamma = 0°$ (or equivalently, $\gamma = 90°$, as shown by the double scale of the abscissa). The degree of anisotropy corresponds to the distance from unity measured on the logarithmic scale of the abscissa. Results obtained by Caltagirone (1976) for the isotropic case ($K^* = 1$) are also shown in this figure. It is observed that the heat transfer is a enhanced for a larger permeability in the vertical direction. It is also observed that the Nusselt number encounters a drastic increase at $K^* \sim 2.5$-3. This peculiar behavior corresponds to the occurence of secondary convective cells at the bottom of the annulus (see Figure 2(a)).

The influence of the angular position γ of the principal axes on the flow and temperature fields is now considered. In Figure 5, the flow (at right) and temperature (at left) fields are shown for $Ra^* = 150$, $K^* = 0.25$ and $\gamma = 0°$, 30°, 45°, 70° and 90°. By comparing the cases 5b,c,d with 5a,e, one can deduce that the anisotropy does not effect equally the two main or primary cells for $\gamma \neq 0°$ or 90°. For $0° < \gamma < 90°$, the left cell becomes stronger and extends over a larger part of the flow domain which includes the inner boundary, thus producing a net circulating flow ($\psi_1 \neq 0$). This net circulating flow is a function of γ as well as of the degree of anisotropy characterizing the porous medium. It is observed that the net circulating flow ceases and that the original symmetry with respect to the vertical diameter reappears when γ reaches 90°. The sequence Figure 5(a-c) shows how the primary cells gradually absorb the secondary cells with departing from zero.

Figure 6 shows the net circulating flow ψ_1 obtained at an angle $\gamma = 45°$, as a function of K^*, for $Ra^* = 100$, 150 and 200. As a consequence of the particular definition of the Rayleigh number, equation (12), and of the logarithmic scale chosen for K^*, a centro-symmetry (or symmetry with respect to the point $\psi_1 = 0$, $K^* = 1$) is found for all the curves in this figure. The centro-symmetry exists only for the particular value $\gamma = 45°$. Another scale for K^*, corresponding to $\gamma = -45°$, is also given in the same figure.

The effect of the inclination angle of the principal axes on the heat transfer is illustrated on Figure 7 where Nu is given as a function of γ for $Ra^* = 100$, 150 and 200. In that figure, Nu is a monotonically increasing function of γ for all the

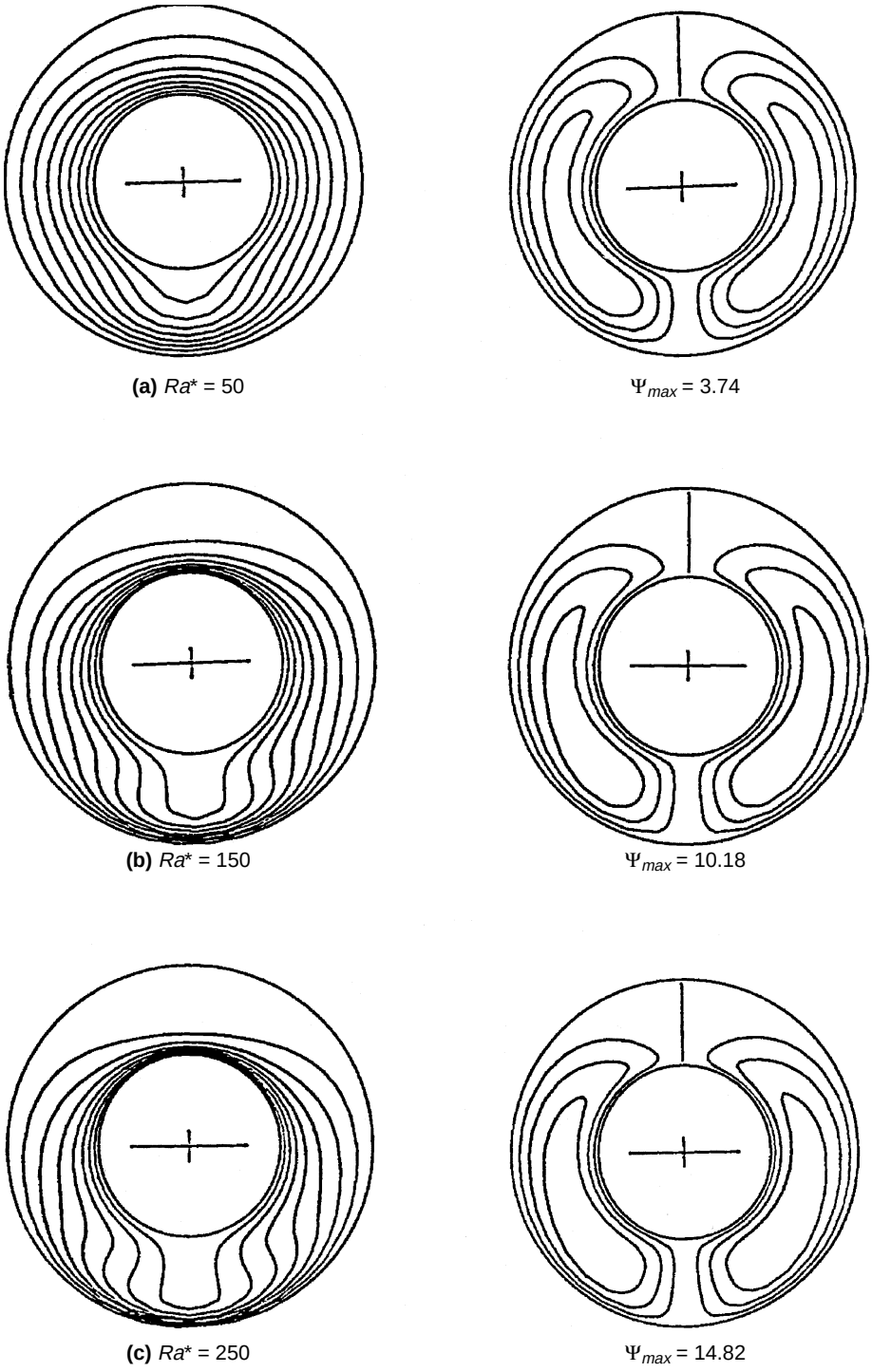

Figure 3.
Flows and temperature fields at different Rayleigh number Ra^*, for $K^* = 0.25$ and $\gamma = 0$

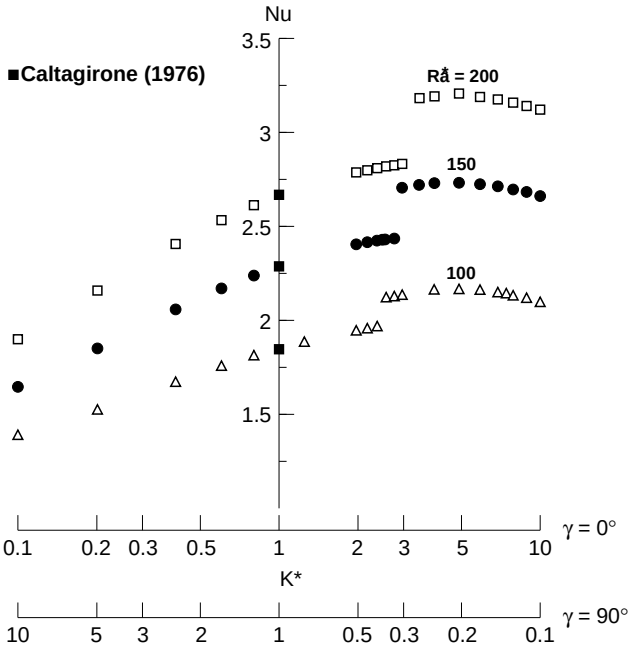

Figure 4.
Nusselt number *Nu* function of the permeability ratio of K^*, for Ra^* = 100, 150 and 200

curves. The three horizontal lines correspond to the values of *Nu* for the isotropic case $K^* = 1$, those values being unaffected by the angle γ and being the same as those of Figure 7 for $K^* = 1$. It is seen that those horizontal lines cross their corresponding anisotropic curves in the neighborhood of $\gamma = 45°$.

As mentioned earlier, the net circulating flow ψ_1 results from the loss of symmetry when $\gamma \neq 0°$ or 90°. In Figure 8, ψ_1 is shown as a function of γ for Ra^* = 100, 150 and 200 while K^* is maintained equal to 0.25. The curves are not symmetrical with respect to 45°. With γ increasing from 0° to 90°, ψ_1 increases to reach a maximum at a value of γ below 40° for the $Ra^* = 200$ curve. It then decreases steadily to reach zero at $\gamma = 90°$.

Conclusions

The problem of a horizontal anisotropic porous annulus with isothermal boundary conditions applied on both inner and outer boundaries has been investigated. The anisotropy considered concerns exclusively the permeability.

Results indicate that for an arbitrary inclination of the principal axes which differs from the horizontal (or vertical) direction, no symmetry of the flow and temperature fields exists with respect to the vertical diameter. In the absence of symmetry, a net circulating flow occurs around the annulus with the maximum value reached when the principal axis, corresponding to the maximum permeability, at ~40° with respect to the vertical diameter, for the Rayleigh numbers considered in this study.

When the principal axes are in the vertical (horizontal) direction, symmetric flow and temperature fields are obtained. A small permeability in the horizontal

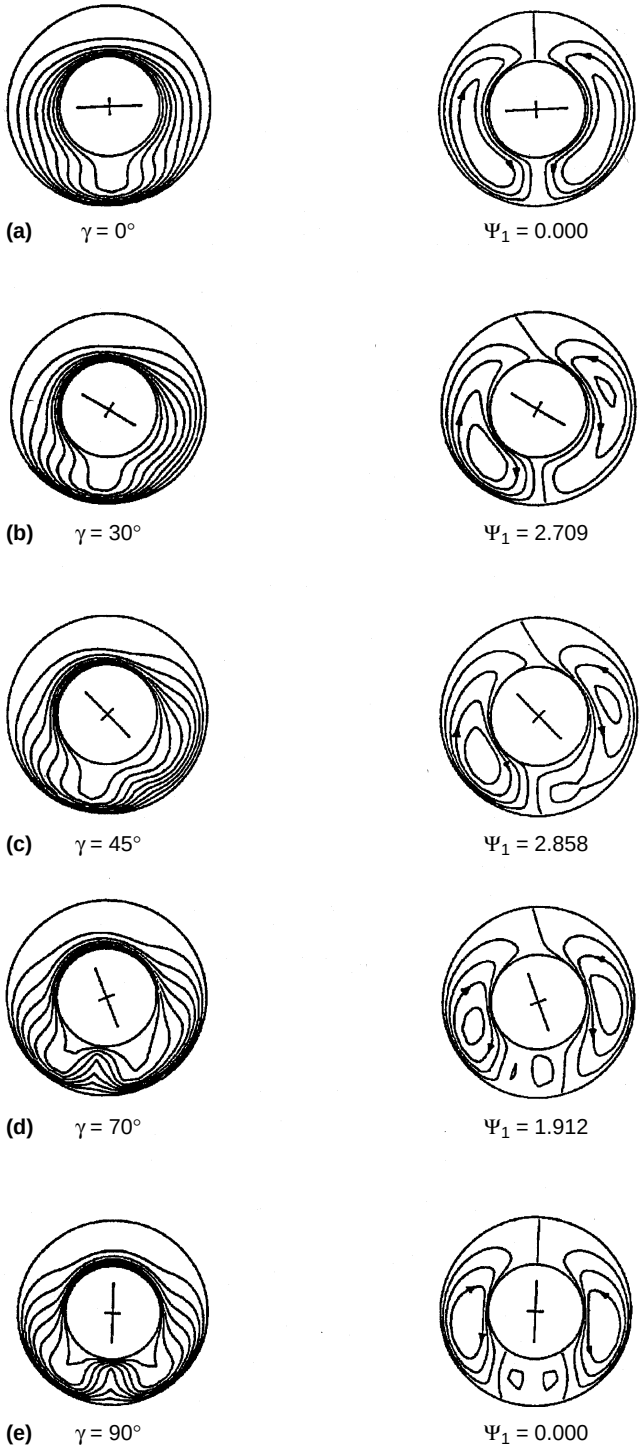

Figure 5.
Effect of the inclination angle γ on the flow (at right) and temperature (at left) fields for $Ra^* = 150$ and $K^* = 0.25$

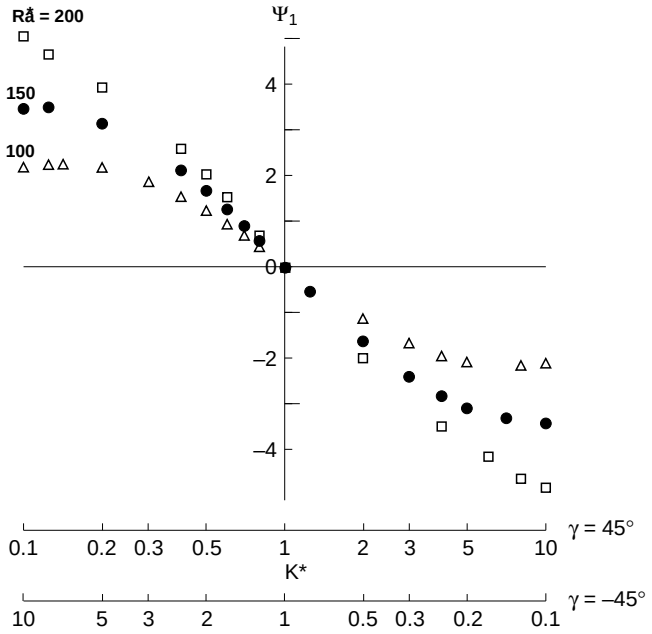

Figure 6.
Net circulating flow ψ_1 function of the permeability ratio K^*, for Ra^* = 100, 150 and 200

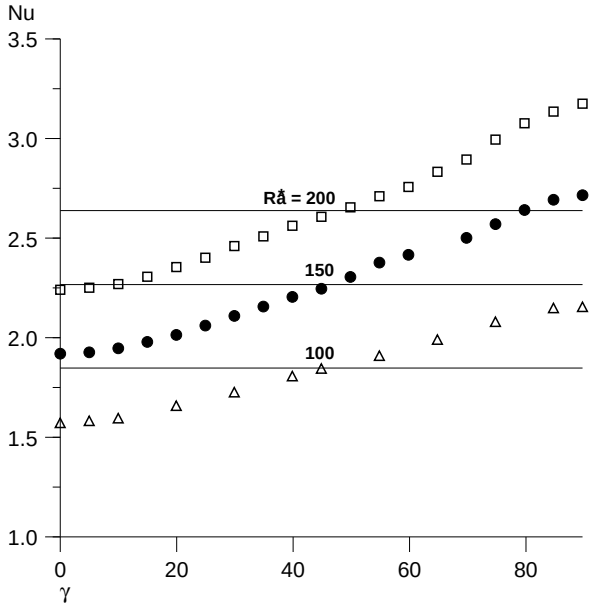

Figure 7.
Nusselt number Nu function of the inclination angle γ for Ra^* = 100, 150 and 200 (K^* = 0.25)

direction enhances the heat transfer and promotes the occurrence of additional cells in the unstable layer at the lower part of the annulus, in a way comparable to a radius ratio decreasing toward unity.

Finally, it has been shown in the Appendix that the effect of anisotropy in permeability is equivalent to the one of a magnetic field acting in the direction

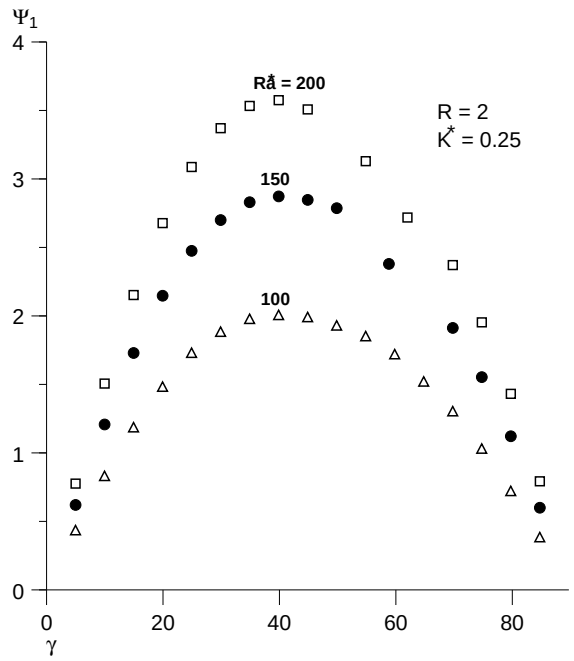

Figure 8.
Net circulating flow ψ_1 function of the inclination angle γ ($K^* = 0.25$)

of the maximum permeability, with the restrictions that the flow stays two-dimensional and that the induced magnetic field due to the fluid motion may be neglected, as well as the Joule dissipation of heat.

References

Bear, J. (1972), *Dynamics of Fluids in Porous Media*, Elsevier, New York, NY.

Burns, P.J., Chow, L.C. and Tien, C.L. (1977), "Convection in vertical slot filled with porous insulation", *Int. J. Heat Transfer*, Vol. 20, pp. 919-26.

Caltagirone, J.P. (1976), "Thermoconvective instabilities in a porous medium bounded by two concentric cylinders", *J. Fluid Mech.*, Vol. 76, pp. 337-62.

Castinel, G. and Combarnous, M. (1977), "Natural convection in an anisotropic porous layer", *Int. Chemical Engineering*, Vol. 17, pp. 605-14.

Chang, W.J. and Hsiao, C.F. (1993), "Natural convection in a vertical cylinder filled with anisotropic porous media", *Int. J. Heat Mass Transfer*, Vol. 36, pp. 3361-7.

Degan, G. and Vasseur, P. (1996), "Natural convection in a vertical slot filled with an anisotropic porous medium with oblique principal axes", *Num. Heat Transfer*, Vol. 30, Part A, pp. 392-412.

Degan, G. and Vasseur, P. (1997), "Boundary layer regime in a vertical porous layer with anisotropic permeability and boundary effects", *Int. J. Heat Fluid Flow*, Vol. 18, pp. 344-3.

Degan, G., Vasseur, P. and Bilgen, E. (1995), "Convective heat transfer in a vertical anisotropic porous layer", *Int. J. Heat Mass Transfer*, Vol. 38, pp. 1975-87.

Ephere, J.F. (1977), "Criterion for the appearance of natural convection in an anisotropic layer", *Int. Chemical Engineering*, Vol. 17, pp. 615-6.

Garandet, J.P., Alboussiere, T. and Moreau, R. (1992), "Buoyancy driven convection in a rectangular enclosure with a transverse magnetic fluid", *Int. J. Heat Mass Transfer*, Vol. 35, pp. 741-8.

Kaviany, M. (1986), "Non-Darcian effects on natural convection in porous media confined between horizontal cylinders", *Int. J. Heat Mass Transfer*, Vol. 29, pp. 1513-19.

Kvernvold, O. and Tyvand, P.A. (1979), "Nonlinear thermal convection in anisotropic porous media", *J. Fluid Mech.*, Vol. 90, pp. 609-24.

Nield, D.A. and Bejan, A. (1992), *Convection in Porous Media*, Springer Verlag, New York, NY.

Ni, J. and Beckermann, C. (1991), "Natural convection in a vertical enclosure filled with anisotropic porous media", *J. Heat Transfer*, Vol. 113, pp. 1033-7.

Ni, J., Beckermann, C. and Smith, T.F. (1993), "Effect of an electromagnetic field on natural convection in porous media, ASME HTD", *Fundamentals of Heat Transfer in Electromagnetic, Electrostatic and Acoustic Fields*, Vol. 248, pp. 23-33.

Patil, P.R., Parvathy, C.P. and Venkatakrishnan, K.S. (1989), "Thermohaline instability in rotating anisotropic porous medium", *App. Sci. Res.*, Vol. 46, pp. 73-88.

Appendix

For a two-dimensional frame with insulated boundaries, the electromagnetic or Lorentz body force (by unit volume) acting on a conducting fluid subjected to a magnetic field reduces to (Garandet *et al.* (1992)):

$$\frac{1}{\rho_0}\vec{J}'\times\vec{B}'=\frac{\sigma_m}{\rho_0}(\vec{V}'\times\vec{B}')\times\vec{B}' \tag{A1}$$

where σ_m is the electrical conductivity, $\vec{J}'$, the electrical current and $\vec{B}'$, the imposed magnetic field. For the case of a porous medium saturated with a conductive fluid, V' becomes the filtration velocity.

If $\vec{B}'$ is normal to the two-dimensional plane (r, φ) considered in the present article, i.e. if $\vec{B}' = (0, 0, B')$, then the right hand side of (A1) reduces to:

$$-\frac{\sigma_m}{\rho_0}(\vec{V}'\times\vec{B}')\times\vec{B}'=-\left(\frac{\sigma_m B'^2}{\rho_0}\right)\vec{V}' \tag{A2}$$

Thus the effect of the magnetic field is equivalent to an added isotropic Darcy resistance. This fact has already been brought to attention by Ni *et al.* (1993).

If $\vec{B}'$ is lying in the (r, φ) plane, and having an angle γ with respect to the origin, i.e. if $\vec{B}' = (B' \cos\beta, -B' \sin\beta, 0)$, then the equation (A1) may be expressed as:

$$\left(\frac{\sigma_m B'^2}{\rho_0}\right)\begin{bmatrix}\sin^2\beta & \frac{\sin 2\beta}{2}\\ \frac{\sin 2\beta}{2} & \cos^2\beta\end{bmatrix}\begin{Bmatrix}u'\\ v'\end{Bmatrix} \tag{A3}$$

the second order tensor in (A3) being equivalent to the added resistivity tensor due to anisotropy, equation (3). The coefficient $\sigma_m B'^2/\rho_0$ becomes the Hartman number to the square, $Ha^2 = \vec{B}'^2 K\sigma_m/\mu$ and replaces the coefficient $(1 - K^*)$ in equation (3a).

Of course, a third direction z is always involved in real flow situations and one has to keep in mind that the equivalence found in (A2) or (A3) does not consider that direction.